The electrical and optical anisotropy of rhenium-doped WSe_2 single crystals

2005 J. Phys.: Condens. Matter 17 3575

(http://iopscience.iop.org/0953-8984/17/23/010)

INSTITUTE OF PHYSICS PUBLISHING JOURNAL OF PHYSICS: CONDENSED MATTER

J. Phys.: Condens. Matter **17** (2005) 3575–3583 doi:10.1088/0953-8984/17/23/010

The electrical and optical anisotropy of rhenium-doped WSe_2 single crystals

S Y Hu[1], M C Cheng[1], K K Tiong[1,3] and Y S Huang[2]

[1] Department of Electrical Engineering, National Taiwan Ocean University, Keelung 202, Taiwan
[2] Department of Electronic Engineering, National Taiwan University of Science and Technology, Taipei 106, Taiwan

E-mail: b0114@mail.ntou.edu.tw

Received 9 December 2004, in final form 6 May 2005
Published 27 May 2005
Online at stacks.iop.org/JPhysCM/17/3575

Abstract

Single crystals of rhenium-doped WSe_2 with large edge plane have been grown by the chemical vapour transport method using bromine as the transporting agent. From the x-ray diffraction patterns, both the doped and undoped crystals are found to crystallize in the 2H structure. The role of rhenium in affecting both the electrical and optical properties of the WSe_2 crystals is examined. The thicker Re-doped WSe_2 samples enable easier exploration of the electrical and optical anisotropies of the materials both parallel and perpendicular to the crystal $\boldsymbol{c}$-axis. The samples are n-type in nature from Hall measurements and the conductivity anisotropy decreases drastically as a result of doping. Photovoltage measurements revealed that both undoped and Re-doped WSe_2 are indirect semiconductors. The indirect band gap of the doped sample showed considerable red shift compared with the undoped sample and also exhibited anisotropy along and perpendicular to the $\boldsymbol{c}$-axis. The anisotropy in the band gap is attributed to crystal anisotropy, which was also studied via the polarization-dependent electrolyte electroreflectance measurements taken along the van der Waals plane ($\boldsymbol{E} \perp \boldsymbol{c}$; $\boldsymbol{k} \parallel \boldsymbol{c}$) and the as-grown edge plane ($\boldsymbol{E} \perp \boldsymbol{c}$, $\boldsymbol{E} \parallel \boldsymbol{c}$; $\boldsymbol{k} \perp \boldsymbol{c}$). The strong dependence of excitonic transitions A and B on polarization compared with that of the undoped samples.

1. Introduction

Tungsten diselenide is a diamagnetic indirect semiconductor which belongs to the family of group VIB layer-type transition metal dichalcogenides [1–3], TX_2, where T = Mo or W and X = S or Se. WSe_2 compounds have drawn considerable attention due to their technological importance as a lubricant [4], catalyst [5], battery cathodes [6], etc. Recently, WSe_2 has been

[3] Author to whom any correspondence should be addressed.

reported to be a potential candidate for application in high-mobility field-effect transistors [7]. The material also exhibits characteristics of extreme anisotropy in optical, electrical and mechanical properties along and perpendicular to the van der Waals (VdW) planes [1–3]. The anisotropy of the semiconductor is a result of the sandwich structure of X–T–X layers interacting with each other, loosely bonded by the weak van der Waals forces [1–3, 8]. The intralayer bonding is thought to be part ionic and part covalent, with the latter being dominant [3, 8]. The bonding anisotropy defines the exclusive morphology of these crystals as thin, elastic and easy-to-cleave platelets that display good cleavage properties parallel to the layers, which can be exploited to obtain thin single specimens. Recent efforts in studying the influence of the anisotropic electrical and optical properties of TX_2 layered-type transition metal dichalcogenides [9–12] have been implemented by doping the samples with rhenium. It appears that the addition of a small amount of rhenium can promote the growth of a sample with extended edge plane. The larger surface areas of the VdW and edge planes facilitate sufficient working surfaces for the study of the electrical and optical anisotropic properties of the crystals which are thus far difficult to achieve due to the relatively thin undoped 2H-WSe_2 [3, 13].

In this work, we report the electrical and optical anisotropic characterization of Re-doped WSe_2 single crystals. Single crystals of WSe_2 doped with Re were grown by the chemical vapour transport method using bromine as the transporting agent. Undoped WSe_2 has also been grown for the purpose of comparison. The electrical conductivity and Hall measurements perpendicular and parallel to the c-axis at 300 K were carried out to determine the electrical anisotropy of the crystals. Anisotropy of the indirect band gaps parallel and perpendicular to the c-axis was examined by photovoltage measurements at 300 K. Optical anisotropy of excitons A and B was studied using the polarized electrolyte electroreflectance (EER) measurements. The role of rhenium in affecting the electrical and optical anisotropies of the sample will be examined.

2. Crystal growth

Re-doped and undoped single crystals of WSe_2 were grown by the chemical vapour transport method, using Br_2 as the transporting agent. The total charge used in each growth experiment was about 10 g. A stoichiometrically determined weight of the doping material (∼0.5% nominal concentration) was added in the hope that it would be transported at a rate similar to that of W. Prior to the crystal growth, quartz tubes containing bromine and the elements (W: 99.99%; Re: 99.99% and Se: 99.999%) were evacuated and sealed. The quartz tube was placed in a three-zone furnace and the reaction took place in the evacuated tube at a temperature of 900 °C for several days. Figure 1 shows a photograph of an as-grown crystal taken at an angle to the edge. The crystal edge is hexagonal in shape and is of typical dimensions: $10 \times 5\ mm^2$ surface area with a thickness of 1.5 mm.

All obtained samples were confirmed to be single-phase materials of 2H structure by a Rigaku RTP 300RC x-ray diffractometer with Cu Kα as the line source ($\lambda = 1.542$ Å). This is quite different for TS_2 [11, 12, 14] materials doped with Re, where 2H to 3R polytype transformation has been demonstrated.

3. Results and discussion

3.1. Conductivity and Hall measurements

For the electrical characterization and Hall measurements, selected samples were cut into rectangular shape (∼$1.5 \times 2 \times 0.3\ mm^3$ for the doped sample and ∼$1.5 \times 2 \times 0.04\ mm^3$ for the undoped sample) and electrical connections to the crystal were made by attaching gold wires

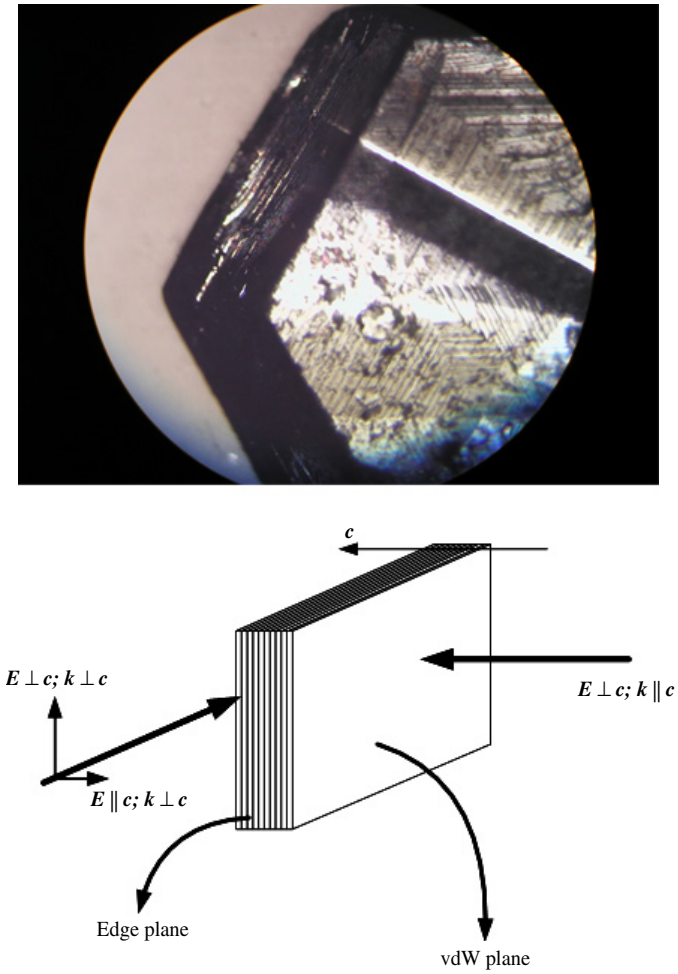

Figure 1. Photograph of an as-grown Re-doped WSe_2 single crystal showing the exposed VdW and edge plane surfaces. The experimental polarization configurations are as shown.

(This figure is in colour only in the electronic version)

to the crystal surface (VdW or edge planes) by means of conducting silver paint. Electrical currents were applied perpendicular or parallel to the *c*-axis at 300 K for the determination of the room-temperature electrical anisotropies of the doped and undoped samples.

The results of the electrical and Hall measurements are summarized in table 1. We emphasize that the observation of some discrepancy in the conductivity for both doped and undoped samples from different growth batches or even from the same batch is quite common. This is most probably due to the uncontrollable variation of the crystal stoichiometry during growth [15–17]. Room-temperature Hall measurements indicate n-type semiconducting behaviour for both undoped and Re-doped WSe_2 single crystals. In our growth attempts, we found that utilizing bromine as the transporting agent always resulted in n-type crystals regardless of the types of dopant used in the doping process. This result differs somewhat from that of [15], where p(n)-type $MoSe_2$ crystals were grown using niobium(rhenium) as dopant and bromine as the transporting agent, but agrees with the more recent work of [17]. A probable

Table 1. Electrical transport properties of Re-doped WSe_2 and undoped WSe_2 single crystals at 300 K.

Materials	WSe_2	Re-doped WSe_2
Type	n	n
Conductivity, $\sigma_\perp$ (Ω^{-1} cm^{-1})	0.11	1.06
Conductivity, $\sigma_\parallel$ (Ω^{-1} cm^{-1})	9.13×10^{-5}	2.66×10^{-2}
Conductivity anisotropy $\frac{\sigma_\perp}{\sigma_\parallel}$	~1205	~40
Carrier concentration, n (cm^{-3})	7.3×10^{15}	1.02×10^{17}
Mobility, $\mu_{H_\perp}$ (cm^2 V^{-1} s^{-1})	95	65
Mobility, $\mu_{H_\parallel}$ (cm^2 V^{-1} s^{-1})	—	1.63

reason as pointed out by [16] is the compensating effects of the transport agent. Comparing our present investigation with that of [16], we can infer that the transporting property of bromine is similar to that of chlorine. We did not analyse the crystals further for halogen contamination as our focus is on the doping effect on the electrical and optical anisotropies of the material.

The important parameter in differentiating the doped samples from the undoped ones is the conductivity anisotropy, which is defined to be $\frac{\sigma_\perp}{\sigma_\parallel}$, where $\sigma_\perp$ and $\sigma_\parallel$ refer to conductivities perpendicular and parallel to the c-axis, respectively. From table 1, we see that the pure WSe_2 crystal exhibits extreme conductivity anisotropy along and perpendicular to the c-axis. Our measurements give $\frac{\sigma_\perp}{\sigma_\parallel} \approx 1205$ for the pure sample. For the case of a doped sample, the excess free carriers provided by the rhenium dopant can enhance the conductivity across the van der Waals gap considerably. From table 1, we have $\frac{\sigma_\parallel|_{\text{doped}}}{\sigma_\parallel|_{\text{undoped}}} \approx 291 \gg \frac{\sigma_\perp|_{\text{doped}}}{\sigma_\perp|_{\text{undoped}}} \approx 9.64$. The much larger increase in $\sigma_\parallel$ for the doped sample results in a drastic drop of the conductivity anisotropy to ~40. This sharp decrease in $\frac{\sigma_\perp}{\sigma_\parallel}$ as a result of doping is found to be an inherent characteristic property of compounds with a layered structure and has been observed previously [10].

From the room-temperature Hall measurements for both the doped and undoped WSe_2 crystals, the carrier concentration $n = \frac{1}{|eR_H|}$ can be determined. The carrier concentration evaluated from Hall measurements shows a marked increase for the Re-doped sample. Together with the conductivity measurement, the room-temperature mobility (μ) of the doped and undoped samples can be evaluated. In the case of Re-doped WSe_2, we are able to determine the mobility parallel ($\mu_\parallel$) and perpendicular ($\mu_\perp$) to the c-axis, while for the undoped sample only $\mu_\perp$ can be determined. Our measurements are consistent with the previous reported values where doping generally resulted in a lowering of $\mu_\perp$ [9, 10]. This means that carrier concentration is the dominant factor in enhancing $\sigma_\perp$ of the doped indirect semiconducting layered compounds. The electrical transport measurements on the doped sample show that the conductivity anisotropy is due to the anisotropy in the mobility of the charge carriers parallel and perpendicular to the c-axis ($\frac{\mu_\perp}{\mu_\parallel} \approx \frac{\sigma_\perp}{\sigma_\parallel} \approx 40$) as the charged carriers have larger effective mass along the c-axis [3, 18, 19]. The relation $\frac{\mu_\perp}{\mu_\parallel} \approx \frac{\sigma_\perp}{\sigma_\parallel}$ should also be valid for the case of the undoped sample. Using this relation, we come to the conclusion that $\mu_\parallel$ should increase with doping in order to cause such a drastic change in the conductivity anisotropy. The increase in $\mu_\parallel$ due to doping is a direct consequence of the enhancement of the electrical conductivity across the van der Waals gap.

3.2. Photovoltage measurements

The experimental set-up for the photovoltage measurements has been described elsewhere [18]. The energy dependences of the relative photovoltage measurements for Re-doped and undoped

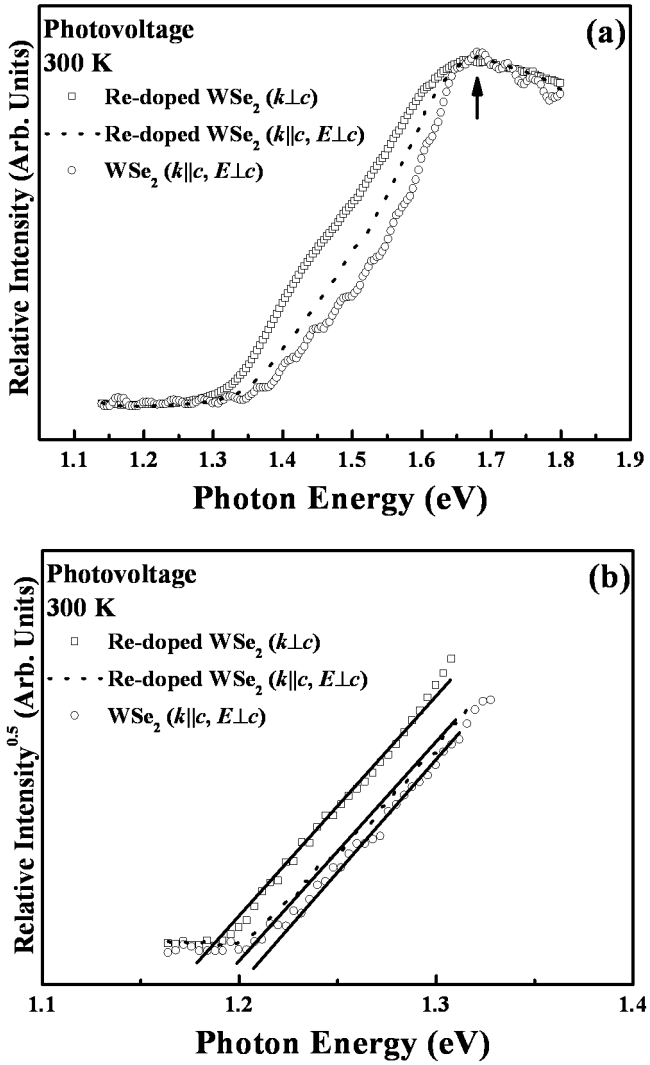

Figure 2. (a) Relative photovoltage spectra for Re-doped WSe_2 and undoped WSe_2 single crystals at 300 K. (b) Square root of the relative photovoltage for Re-doped WSe_2 and undoped WSe_2 single crystals for the determination of the indirect band gap.

WSe_2 are shown in figure 2(a). For the Re-doped sample, measurements both parallel and perpendicular to the c-axis were performed. The photovoltage increases from ∼1.13 to ∼1.67 eV and then decreases in the higher photon energy region. The measurements indicated that a broad peak occurred at ∼1.67 eV as indicated by an arrow. The square root of the relative photovoltage depends linearly [20, 21] on the photon energy $h\nu$ in the range 1.2–1.4 eV as indicated in figure 2(b). This shows an indirect transition with a band edge at the intercept of the plot. The indirect band gap of WSe_2 parallel to the c-axis is fitted to be $E_{\parallel}^{\mathrm{ind}} = 1.20 \pm 0.01$ eV. The indirect band gaps parallel and perpendicular to the c-axis of the Re-doped WSe_2 red shifted and exhibited indirect band gap anisotropy. The indirect band gap for the Re-doped sample parallel to the c-axis (VdW plane) is fitted to be $E_{\parallel}^{\mathrm{ind}} = 1.18 \pm 0.01$ eV,

while perpendicular to $\boldsymbol{c}$-axis (edge plane), $E_{\perp}^{\mathrm{ind}} = 1.15 \pm 0.01$ eV. The red shift in $E_{\parallel}^{\mathrm{ind}}$ by 20 meV is attributed to a small concentration of rhenium dopant in the doped sample, while the measured anisotropy which is defined as $\Delta E = E_{\parallel}^{\mathrm{ind}} - E_{\perp}^{\mathrm{ind}} = 30$ meV is attributed to crystal anisotropy as a result of interlayer van der Waals interaction. The same mechanisms can also affect the direct gap of WSe_2 and will be examined closer with the EER experiments. A comparison of the photovoltage peak centred around 1.67 eV with that of the exciton A signal in the EER experiments (which will be presented later) indicates a strong absorption at the direct interband transitions around the critical point.

3.3. Electrolyte electroreflectance measurements

For the EER experiments, maximum size crystals of Re-doped and undoped WSe_2 were selected. The EER measurements were taken on a completely computerized system for modulation spectroscopy described elsewhere [22, 23]. Reflectivities from both VdW planes ($\boldsymbol{k} \parallel \boldsymbol{c}$; $\boldsymbol{E} \perp \boldsymbol{c}$) and edge planes ($\boldsymbol{k} \perp \boldsymbol{c}$; $\boldsymbol{E} \perp \boldsymbol{c}$ and $\boldsymbol{E} \parallel \boldsymbol{c}$) for Re-doped WSe_2 were measured, with $\boldsymbol{E}$, $\boldsymbol{k}$ the electric vector and wavevector, respectively, of the incident light and $\boldsymbol{c}$ the long axis of the crystal. For the undoped sample, only reflection off the VdW plane can be performed because of the overly thin undoped sample. The experimental polarization schemes are shown in figure 1, together with a photograph of the as-grown Re-doped WSe_2 showing the exposed VdW and edge plane surfaces.

Displayed by the dotted curves in figures 3(a) and (b) are the EER spectra near the direct band-edge over the range 1.4–2.4 eV at room temperature. The nature of the line shape indicates that the energy separation between the A and B transitions is due to the spin–orbit splitting of the top of the valence band corresponding to the smallest direct transition at the $\boldsymbol{K}$ points of the Brillouin zone [18]. The experimental curves have been fitted to a functional form appropriate for excitonic transitions that can be expressed as a Lorentzian line shape function of the form [24]

$$\frac{\Delta R}{R} = \mathrm{Re}\left[\sum_{i=1}^{m} C_i \mathrm{e}^{j\phi_i}(E - E_i + j\Gamma_i)^{-2}\right] \tag{1}$$

where C_i and ϕ_i are the amplitude and phase factors, E is the incident photon energy, E_i is the energy of the transition, and Γ_i is the line shape broadening parameter. The least squares fits using equation (1) are shown as solid curves and the obtained values of E_i are indicated as arrows. The assignment of the features follows that of the experimental results of Liang [3].

The $\boldsymbol{k} \parallel \boldsymbol{c}$; $\boldsymbol{E} \perp \boldsymbol{c}$ polarized EER spectra for the undoped and Re-doped WSe_2 are displayed in figure 3(a), while the $\boldsymbol{k} \perp \boldsymbol{c}$; $\boldsymbol{E} \perp \boldsymbol{c}$ and $\boldsymbol{E} \parallel \boldsymbol{c}$ polarized EER spectra for the Re-doped WSe_2 sample are displayed in figure 3(b). The observed features were assigned as A, B and A′ by comparing and referring to the absorption spectrum of Liang [3] and the wavelength-modulated reflection (WMR) spectrum of Anedda *et al* [25]. The observed differences between the EER spectra of undoped and Re-doped samples can be attributed to the presence of rhenium impurity or the crystal anisotropy. Table 2 summaries the peak positions of the observed features as recorded in figures 3(a) and (b) together with the data of the 5 K absorption spectrum of Liang [3] and the 10 K WMR spectrum of Anedda *et al* [25] for reference and comparison.

In this section, we will focus our discussion on the role of rhenium dopant in affecting the change in the optical anisotropy of the Re-doped WSe_2. By referring to the spectrum of the $\boldsymbol{k} \parallel \boldsymbol{c}$ configuration for the undoped WSe_2 in figure 3(a), the A exciton series appeared sharper, with the structure resolved into A_1 and A_2 features at $E_{A_1} = 1.630 \pm 0.003$ eV and $E_{A_2} = 1.658 \pm 0.003$ eV. The direct band gap $E_g^{\mathrm{d}} = 1.667 \pm 0.003$ eV and the exciton binding

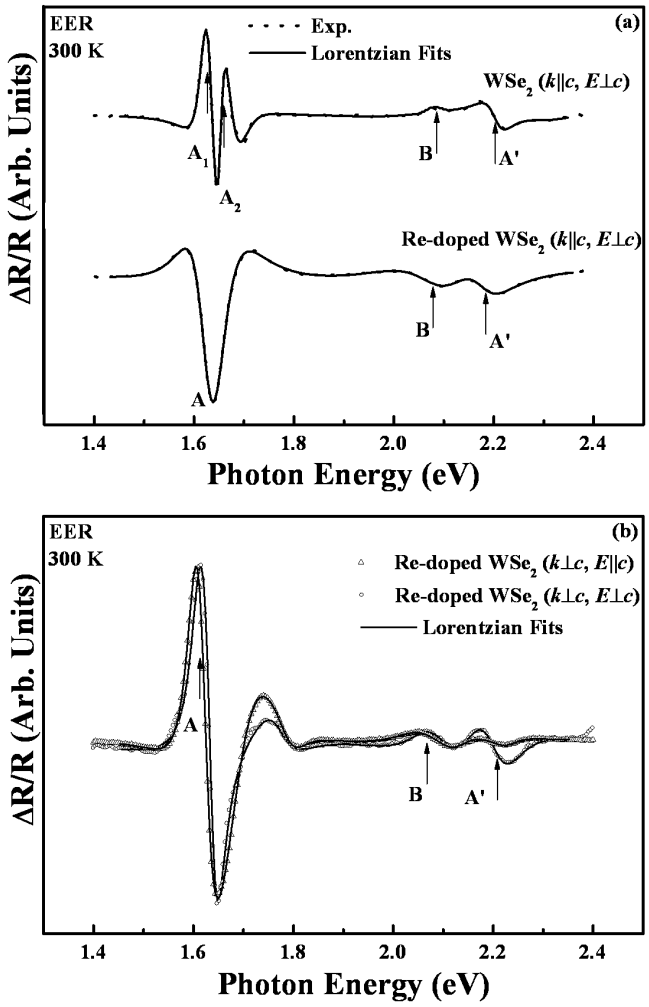

Figure 3. (a) The EER spectra of undoped and Re-doped WSe_2 single crystals over the energy range 1.4–2.4 eV for the VdW ($k \parallel c$) plane. (b) The polarization-dependent EER spectra of a Re-doped WSe_2 single crystal over the energy range 1.4–2.4 eV for the edge ($k \perp c$) plane. The solid curves are the least-squares fits to a Lorentzian lineshape expression which yield the excitonic transition energies as indicated by the arrows.

energy of $R = 37.3 \pm 3$ meV can be deduced using the Mott–Wannier exciton relation [3, 19]. Exciton B was also detected as a weak and broadened feature at 2.085 ± 0.005 eV. The EER spectrum of the Re-doped sample for the same polarization configuration gives a much broader feature denoted as A at 1.632 ± 0.003 eV with no observable higher bands. The broadening linewidth of the exciton A feature is most likely due to impurity scattering and deterioration of the crystal quality. The feature related to exciton B is detected at 2.078 ± 0.005 eV and is similar to that of the undoped sample. The energy of the spin–orbit splitting for both Re-doped and undoped WSe_2 is comparable at around 450 meV, which is consistent with the finding that both samples are of the same 2H-polytype, in contrast with Re-doped MoS_2 where a transformation to 3R-polytype has taken place, resulting in a significant shrinkage in the spin–orbit splitting [11]. The A′ feature, which is related to higher interband transition, showed a

Table 2. Positions of the spectral features from the EER spectra of undoped and Re-doped WSe_2 single crystals as depicted in figures 3(a) and (b). The data from [3] and [23] are also listed for comparison.

	EER (300 K)				Absorption[a] (5 K)	WMR[b] (10 K)
	WSe_2 (eV)	Re-doped WSe_2 (eV)			2H-WSe_2 (eV)	2H-WSe_2 (eV)
	$\boldsymbol{k} \parallel \boldsymbol{c}$	$\boldsymbol{k} \parallel \boldsymbol{c}$	$\boldsymbol{k} \perp \boldsymbol{c}$		$\boldsymbol{k} \parallel \boldsymbol{c}$	$\boldsymbol{k} \parallel \boldsymbol{c}$
Feature	$\boldsymbol{E} \perp \boldsymbol{c}$	$\boldsymbol{E} \perp \boldsymbol{c}$	$\boldsymbol{E} \perp \boldsymbol{c}$	$\boldsymbol{E} \parallel \boldsymbol{c}$	$\boldsymbol{E} \perp \boldsymbol{c}$	$\boldsymbol{E} \perp \boldsymbol{c}$
A_1	1.630 ± 0.003	1.632 ± 0.003	1.618 ± 0.003	1.614 ± 0.003	1.694	1.714
A_2	1.658 ± 0.003	—	—	—	—	—
B	2.085 ± 0.005	2.078 ± 0.005	2.068 ± 0.005	2.065 ± 0.005	2.174	2.182
A′	2.204 ± 0.005	2.184 ± 0.005	2.212 ± 0.005	2.222 ± 0.005	2.260	2.260

[a] Reference [3].
[b] Reference [23].

much more pronounced red shift of 20 meV for the Re-doped sample. The fitted values of the features are listed in table 2 together with that of [3] and [25] for comparison.

We will now turn our attention to the polarization-dependent EER spectra of the Re-doped WSe_2 as depicted in figures 3(a) and (b). A comparison of the different polarization configurations EER spectra revealed the effect of interlayer van der Waals interaction. From figures 3(a) and (b), the spectra of $\boldsymbol{k} \parallel \boldsymbol{c}$ and $\boldsymbol{k} \perp \boldsymbol{c}$ configurations with $\boldsymbol{E} \perp \boldsymbol{c}$ polarization for Re-doped WSe_2 showed the measured difference for the peak positions of exciton A to be 14 meV and that of exciton B to be 10 meV. These values are comparable to the observable shift as described by Chaparro *et al* [13] to be that between smooth (VdW-plane) and corrugated (edge-plane) regions. The shift is attributed to crystal anisotropy [13] which can affect the dielectric constants and exciton effective masses parallel and perpendicular to the $\boldsymbol{c}$-axis. For WSe_2, the dielectric constants perpendicular and parallel to the $\boldsymbol{c}$-axis are $\varepsilon_\perp = 12.7$ and $\varepsilon_\parallel = 4.2$, respectively, while for the exciton effective masses, $m^*_\parallel > m^*_\perp$ [18, 19]. A straightforward analysis making use of the Mott–Wannier exciton relation can readily deduce that $E^{\mathrm{dir}}_\parallel > E^{\mathrm{dir}}_\perp$, in qualitative agreement with our previous experimental observation [11] and that of Chaparro *et al* [13]. The spectra from the edge plane surface ($\boldsymbol{k} \perp \boldsymbol{c}$) with $\boldsymbol{E} \perp \boldsymbol{c}$ and $\boldsymbol{E} \parallel \boldsymbol{c}$ polarizations also showed energy of exciton A at 1.618 ± 0.003 and 1.614 ± 0.003 eV, respectively. The corresponding positions for exciton B are at 2.068 ± 0.005 eV and 2.065 ± 0.005 eV, respectively. It appears that a small red shift of 4 meV is recorded for the exciton A feature in $\boldsymbol{E} \perp \boldsymbol{c}$ and $\boldsymbol{E} \parallel \boldsymbol{c}$ spectra. The measured shift, though small, is consistent by careful repetition of the experiments. The same observation is not that obvious for exciton B as the feature is much weaker and broader than the A feature. A probable origin of this shift may come from the enhancement of the lattice polarizability of the intralayer bonding through doping with rhenium. Under depletion conditions, the excitonic features are expected to increase with increasing electric field (by increasing band-bending). The electric field effect for $\boldsymbol{E} \parallel \boldsymbol{c}$ polarization is larger than for $\boldsymbol{E} \perp \boldsymbol{c}$ polarization. Therefore, we would expect the electric field induced shift of the excitons to be larger for electric field parallel to the $\boldsymbol{c}$-axis. This effect, in general, may be too small to be observable [13]. However, if we can enhance the effect, as in our case, by enhancing the lattice polarizability, the electric field induced anisotropy may be observed.

4. Summary

In summary, we have studied the electrical and optical anisotropic properties of undoped and Re-doped WSe_2 via room-temperature electrical conductivity and Hall measurements and the polarization-dependent EER. The results indicate that the incorporation of a small amount of rhenium into WSe_2 has formed impurity levels. The electrical anisotropy of the doped WSe_2 reduced drastically to ∼40 from that of ∼1205 for the undoped sample. The room-temperature Hall effect measurements showed that the electrical anisotropy is a result of the anisotropy in the electron mobility. The photovoltage measurements indicate an indirect transition for WSe_2 and a red shift of 20 meV in the indirect band gap for Re-doped WSe_2 compared with the undoped sample. By analysing the photovoltage data from the VdW and edge planes, the crystal anisotropy induced shift of 30 meV is deduced for the indirect gap. From the polarized EER spectra with $\boldsymbol{k} \parallel \boldsymbol{c}$; $\boldsymbol{E} \perp \boldsymbol{c}$ configuration for doped and undoped samples, the main influence of rhenium is determined to be acting as an impurity which contributes to the broadening parameter of the features. A comparison of the $\boldsymbol{k} \parallel \boldsymbol{c}$; $\boldsymbol{E} \perp \boldsymbol{c}$ and $\boldsymbol{k} \perp \boldsymbol{c}$; $\boldsymbol{E} \perp \boldsymbol{c}$ EER spectra for Re-doped WSe_2 revealed a crystal anisotropy (interlayer van der Waals interaction) induced shift of ∼14 meV for exciton A and ∼10 meV for exciton B. Finally, the experimental EER spectra of $\boldsymbol{k} \perp \boldsymbol{c}$ with $\boldsymbol{E} \perp \boldsymbol{c}$ and $\boldsymbol{E} \parallel \boldsymbol{c}$ for Re-doped sample point to the possible effect of intralayer electric field induced anisotropy.

Acknowledgments

The authors S Y Hu, M C Cheng and K K Tiong would like to acknowledge the support of the National Science Council of the Republic of China under Project No NSC93-2112-M-019-005. Y S Huang acknowledges the support of the National Science Council of the Republic of China under Project No NSC92-2112-M-011-001.

References

[1] Wilson J A and Yoffe A D 1969 *Adv. Phys.* **18** 193
[2] Beal A R, Knights J C and Liang W Y 1972 *J. Phys. C: Solid State Phys.* **5** 3540
[3] Liang W Y 1973 *J. Phys. C: Solid State Phys.* **6** 551
[4] Lince J R and Fleischauer P D 1987 *J. Mater. Res.* **2** 827
[5] Chianelli R R 1984 *Catal. Rev.-Sci. Eng.* **26** 361
[6] Bouxel J and Brech R A 1986 *Rev. Mater. Sci.* **16** 137
[7] Podzorov V, Gershenson M E, Kloc Ch, Zeis R and Bucher E 2004 *Appl. Phys. Lett.* **84** 3301
[8] Weiser G 1973 *Surf. Sci.* **37** 175
[9] Tiong K K, Huang Y S and Ho C H 2001 *J. Alloys Compounds* **317/318** 208
[10] Tiong K K, Ho C H and Huang Y S 1999 *Solid State Commun.* **111** 635
[11] Tiong K K and Shou T S 2000 *J. Phys.: Condens. Matter* **12** 5043
[12] Tiong K K, Shou T S and Ho C H 2000 *J. Phys.: Condens. Matter* **12** 3441
[13] Chaparro A M, Salvador P, Coll B and Gonzalez M 1993 *Surf. Sci.* **293** 160
[14] Yen P C, Huang Y S and Tiong K K 2004 *J. Phys.: Condens. Matter* **16** 2171
[15] Levy F, Schmid P H and Berger H 1976 *Phil. Mag.* **34** 1129
[16] Koval C A and Olson J B 1987 *J. Electroanal. Chem.* **234** 133
[17] Legma J B, Vacquier G, Traore H and Casalot A 1991 *Mater. Sci. Eng.* B **8** 167
[18] Coehoorn R, Haas C and de Groot R A 1987 *Phys. Rev.* B **35** 6203
[19] Beal A R and Liang W Y 1976 *J. Phys. C: Solid State Phys.* **9** 2459
[20] Huang Y S and Chen Y F 1988 *Phys. Rev.* B **38** 7997
[21] Pankove J I 1975 *Optical Processes in Semiconductors* (New York: Dover) p 38
[22] Aspnes D E 1980 *Optical Properties of Semiconductors* (*Handbook on Semiconductors*) ed M Balkanski (Amsterdam: North-Holland) p 109
[23] Schroder D K 1998 *Semiconductor Material and Device Characterization* 2nd edn (New York: Wiley) p 671
[24] Cardona M, Shaklee K L and Pollak F H 1967 *Phys. Rev.* **154** 696
[25] Anedda A, Fortin E and Raga F 1979 *Can. J. Phys.* **57** 368